Field-Cycled MRI System Design

K. M. Gilbert[1], J. W. Odegaard[1], W. B. Handler[1], T. J. Scholl[1], B. A. Chronik[1]
[1]Physics and Astronomy, University of Western Ontario, London, Ontario, Canada

Introduction: Conventional MRI uses a high-field superconducting magnet to both polarize and subsequently image an object. A field-cycled MRI system differentiates between the polarizing and readout phases of MRI by implementing two separately controllable resistive magnets to perform these tasks: a high-field inhomogeneous polarizing magnet and a low-field homogenous readout magnet [1]. The ability to vary the polarizing field strength and duration allows for greater diversity in T1 contrast between tissues. Performing the acquisition phase at low-field reduces susceptibility artefacts, such as between tissue and medical implants. We also believe that the flexibility in the design of the resistive magnets allows for the development of open, multi-modality systems, combining field-cycled MRI with other imaging modalities such as Positron Emission Tomography (PET) or Single Photon Emission Computed Tomography (SPECT).

A field-cycled MRI pulse sequence is dramatically different from that of conventional MRI. A strong but variable magnetic field is applied initially to magnetize the sample. After a variable length of time, the polarizing field (*Bp*) is rapidly switched off, while a relatively weak magnetic field (*Br*) is applied during readout. The high-field magnetization present in the sample will begin to decay to the low-field equilibrium value, leaving hundreds of milliseconds to acquire a signal. Figure 1 is a schematic of a field-cycled MR gradient-echo pulse sequence. In this abstract, we describe the design of our proposed field-cycled system and discuss the electromagnetic, SNR, and thermal considerations that were taken into account.

Theory: In field-cycled MRI the polarizing and readout fields are different, thus altering the basic SNR equations. We can consider two SNR regimes: coil noise dominance (CND) and body noise dominance (BND) [2]. In our proposed field-cycled MRI system, the readout frequency is on the lower end of the transition regime between CND and BND. In the BND regime, SNR is independent of readout field strength. This suggests that there is little SNR benefit in increasing readout field strengths beyond that necessary to enter the BND regime. In the CND regime, the system noise is dominated by that of the RF coil [3], and the SNR depends on:

$$SNR_{CND} \propto (Br)^{3/4}(Bp)(B1) \qquad \text{[Eq. 1]}$$

where B1 is the r.f. field efficiency. The above SNR dependency was used in optimizing the geometry of our proposed system.

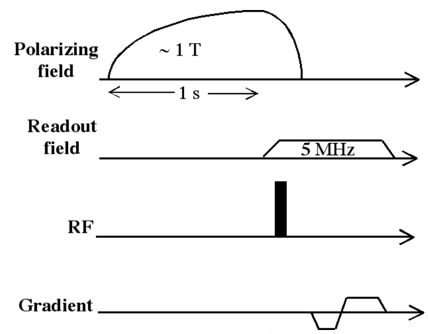

Figure 1: A typical gradient echo pulse sequence for field-cycled MRI. The polarizing pulse can vary in duration and amplitude.

System Design: The polarizing magnet consists of a long thick solenoid that has been modularized by the addition of forced water-cooling plates orthogonal to the longitudinal axis. From the Fabry parameter[4], a dimensionless quantity proportionally to the power efficiency of a solenoid, the geometry of the polarizing magnet can be chosen that will produce the maximum power efficiency for any given inner radius [4]; the absolute field is then limited by the power capabilities of the available amplifier. The readout magnet was designed using a simulated annealing algorithm [5]. A 4-coil readout magnet was chosen because it was found to offer both a lower inductance and weight, with a similar homogeneity (~60 ppm over the 10 cm FOV) and tolerance to displacement as that of a 6-coil magnet. The readout field for our initial prototype was chosen to be 5 MHz (0.12 T). Higher readout frequencies start to enter the BND regime, with diminishing benefits in SNR and increasing difficulty in both magnet cooling and field stability. In the CND regime, we found it to be advantageous in terms of SNR to position the polarizing magnet within the inside of the readout magnet. The inner diameter of the polarizing magnet was limited by the need to allot space for the gradient, shim coils, and RF shield. We investigated both the SNR and thermal trade-offs involved in increasing the outer diameter of the polarizing magnet while increasing the inner diameter of the readout magnet, and arrived at the configuration summarized in Table 1. Both magnets will be powered using 200V, 100A amplifiers; therefore, both were designed as 1.7 Ohm loads at room temperature. This allows for the magnets to present approximately 2 Ohm loads when at equilibrium operating temperatures. Cooling tubes and system supports are positioned between the polarizing and readout magnets.

We have also developed theoretical models to predict, both spatially and temporally, the thermal performance of the magnet system and the influence of forced water-cooling. The number of cooling plates in the polarizing magnet was optimized to limit its equilibrium temperature to less than 150 °C when driven at 100% duty cycle. Table 1 gives the specifications of the system. A schematic of the system currently under construction is shown in Fig. 2.

We developed all of the system design and optimization tools ourselves and we are completing the fabrication of the entire system completely in-house. Once the prototype system has been tested, we will use it to evaluate the potential advantages of field-cycled MRI and the possibility of developing a new field-cycled MRI platform for integration with a PET system.

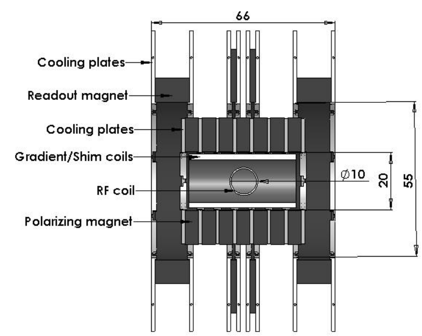

Figure 2: A cross-section of the final design for the field-cycled MRI system. All dimensions are given in centimeters.

Table 1: Specifications of the field-cycled MRI system.

Magnet:	Polarizing	Readout
Field	0.43 T	5 MHz
Inner diameter [cm]	21	56
Outer diameter [cm]	42	72/92
Uniformity	30%	60 ppm
Inductance [mH]	500	430
Resistance [Ω]	1.7	1.4
Cooling plates	8	2/coil
Length [cm]	36	66
Weight [kg]	350	500
Gradient/Shim coil width [cm]	3.5	
r.f. coil diameter [cm]	10	

References:
[1] Macovski *et al.*, Magn. Reson. Med. **30**, 221-230 (1993).
[2] Morgan *et al.*, Magn. Reson. Med. **36**, 527-536 (1996).
[3] Hoult, J. Magn. Reson. **34**, 425-433 (1979).
[4] Montgomery, D. Bruce. Solenoid Magnet Design. New York: John Wiley & Sons, Inc.; 1969.
[5] Aarts, E. Simulated Annealing and Boltzmann Machines. Toronto: Wiley; 1989.